Progesterone-Dependent Induction of Phospholipase C-Related Catalytically Inactive Protein 1 (PRIP-1) in Decidualizing Human Endometrial Stromal Cells

Joanne Muter*, Paul J Brighton*, Emma S Lucas, Lauren Lacey, Anatoly Shmygol, Siobhan Quenby, Andrew M Blanks & Jan J Brosens

Division of Biomedical Sciences (J.M., P.J.B., E.S.L., L.L., S.Q., A.S., A.M.B & J.J.B.), Warwick Medical School, University of Warwick, Coventry, CV4 7AL, United Kingdom.

University Hospitals Coventry and Warwickshire NHS Trust (S.Q., J.J.B), Clifford Bridge Rd, Coventry, CV2 2DX, United Kingdom.

* These authors contributed equally to this work

Abbreviated Title: PRIP-1 in decidualization

Key terms: endometrium, decidualization, PRIP-1, AKT, FOXO1, Ca^{2+} signaling

Word count: 4369

Number of figures and tables: 5 Figures, Antibody List

Corresponding author and person to whom reprint requests should be addressed:

Jan Brosens MD PhD, Division of Biomedical Sciences, Warwick Medical School, University of Warwick, Coventry CV4 7AL, UK – Tel: +44 2476 968704; E-mail: J.J.Brosens@warwick.ac.uk

Disclosure Statement: The authors have nothing to disclose

Abstract

Decidualization denotes the transformation of endometrial stromal cells into specialized decidual cells. In pregnancy, decidual cells form a protective matrix around the implanting embryo, enabling coordinated trophoblast invasion and formation of a functional placenta. Continuous progesterone signaling renders decidual cells resistant to various environmental stressors whereas withdrawal inevitably triggers tissue breakdown and menstruation or miscarriage. Here we show that *PLCL1*, coding phospholipase C-related catalytically inactive protein 1 (PRIP-1), is highly induced in response to progesterone signaling in decidualizing human endometrial stromal cells (HESCs). Knockdown experiments in undifferentiated HESCs revealed that PRIP-1 maintains basal phosphoinositide 3-kinase / AKT activity, which in turn prevents illicit nuclear translocation of the forkhead transcription factor FOXO1 and induction of the apoptotic activator BIM. By contrast, loss of this scaffold protein did not compromise survival of decidual cells. PRIP-1 knockdown did also not interfere with the responsiveness of HESCs to deciduogenic cues, although the overall expression of differentiation markers, such as *PRL*, *IGFBP1* and *WNT4*, was blunted. Finally, we show that PRIP-1 in decidual cells uncouples phospholipase C (PLC) activation from intracellular Ca^{2+} release by attenuating inositol trisphosphate (IP_3) signaling. In summary, PRIP-1 is a multifaceted progesterone-inducible scaffold protein that gates the activity of major signal transduction pathways in the endometrium. It prevents apoptosis of proliferating stromal cells and contributes to the relative autonomy of decidual cells by silencing PLC signaling downstream of G_q-protein-coupled receptors.

Introduction

Decidualization of the endometrium is indispensible for pregnancy (1). The postovulatory surge in progesterone and rising cellular cAMP levels during the mid-luteal phase of the cycle initiate this transformational process (2,3), characterised by the differentiation of stromal cells in the superficial endometrial layer into specialist decidual cells. Continuous progesterone signaling is critical for maintaining and enhancing the decidual phenotype throughout pregnancy (4). In the absence of a viable pregnancy, falling progesterone levels trigger proteolytic breakdown of the superficial endometrial layer, focal bleeding and menstruation or menstruation-like bleeding in the case of miscarriage (5-8). Aberrant decidualization has been implicated in a range of reproductive disorders including endometriosis (9,10), infertility and recurrent pregnancy loss (11-14).

Once the luminal endometrial epithelium is breached, migratory decidualizing stromal cells rapidly encapsulate the invading blastocyst (1,15,16). Emerging evidence indicates that decidual cells play a critical role in embryo biosensoring and selection (17-19). As pregnancy unfolds, decidual cells safeguard the conceptus against various stressors. For example, stress-induced signaling through c-Jun N-terminal kinase (JNK) and p38 pathways is selectively inactivated upon decidualization of human endometrial stromal cells (HESCs) (20). Combined with the induction of various free radical scavengers, silencing of these stress-signaling pathways renders decidual cells extraordinarily resistant to oxidative cell death (21-24). Moreover, circadian oscillations within the endometrium are firmly disabled upon decidualization, further isolating the implanting blastocyst from the maternal environment (25).

This study investigates the role of PRIP-1 [Phospholipase C (PLC)-Related, but catalytically Inactive Protein-1] in decidualizing HESCs. PRIP-1, coded by *PLCL1* (phospholipase C-like 1), is structurally homologous to members of the PLC family although it lacks catalytic activity

(26,27). Like PLC-enzymes, PRIP-1 contains a pleckstrin homology (PH) domain enabling binding of phosphatidylinositol 4,5-bisphosphate (PIP_2) and other phosphoinositides. However, two key amino-acid mutations within the catalytic domain of PRIP-1 ensure that it cannot convert PIP_2 to inositol 1,4,5-trisphosphate (IP_3) and diacylglycerol (DAG) (28). Consequently, PRIP-1 attenuates IP_3-dependent Ca^{2+} release from the endoplasmic reticulum (ER) (29). PRIP-1 also acts as a scaffold protein capable of binding protein phosphatases 1 and 2A (PP1 and PP2A) as well as AKT, a serine/threonine kinase that relays growth factor signaling downstream of phosphoinositide 3-kinase (PI3K) (30,31). The forkhead box protein FOXO1 is a key decidual transcription factor downstream of the PI3K/AKT pathway (32-34). By binding to the progesterone receptor (PGR) and other decidual transcription factors, FOXO1 drives the expression of several decidual marker genes, including *PRL*, *IGFBP1* and *WNT4* (34-36). However, FOXO1 is also important for cell fate decisions and upregulates the pro-apototic Bcl-2 family member BIM, coded by *BCL2L11*, upon withdrawal of progesterone from decidualizing cultures, triggering cell death (37).

Gene deletions in mice highlighted the importance of both Prip-1 and its analogue Prip-2 in reproduction. Double Prip-1/2 deficient mice display reduced litter sizes and exhibit prolonged intervals between litters. Furthermore, mutant female mice have smaller uteri at puberty, spend more time in estrous, and have higher gonadotrophin levels (38). *PRIP-1* has also been identified as a progesterone-responsive gene in the human myometrium (39). Taken together, these findings suggest that PRIP proteins are not only essential for optimal regulation of the hypothalamic–pituitary–gonadal axis but may also play a role in modulating steroid hormone responses in target tissues, such as the uterus.

Here we report that PRIP-1 is strongly induced in decidualizing HESCs in response to progesterone signaling. We show that this scaffold protein not only modulates the activity of

the PI3K/AKT/FOXO1 pathway in undifferentiated HESCs but also acts as a chelator of IP_3 signaling in decidual cells.

MATERIALS AND METHODS

Patient selection and endometrial sampling

The study was approved by the NHS National Research Ethics – Hammersmith and Queen Charlotte's & Chelsea Research Ethics Committee (1997/5065). Subjects were recruited from the Implantation Clinic, a dedicated research clinic at University Hospitals Coventry and Warwickshire National Health Service Trust. Written informed consent was obtained from all participants in accordance with the guidelines in The Declaration of Helsinki 2000. Samples were obtained using a Wallach Endocell^{TM} sampler (Wallach, Trumbull, USA), starting from the uterine fundus and moving downward to the internal cervical ostium. A total of 43 endometrial biopsies were processed for primary cultures in this study. The average age (± SD) of the participants was 35.9 ± 4.7 years. In addition, 98 biopsies were used to measure PRIP-1 expression *in vivo* at mRNA and protein level. All endometrial biopsies were timed between 6 and 10 days after the pre-ovulatory luteinizing hormone (LH) surge. None of the subjects were on hormonal treatments for at least 3 months prior to the procedure.

Primary cell culture

HESCs were isolated from endometrial tissues as previously described (40). Purified HESCs were expanded in culture medium of DMEM/F-12 containing 10% dextran-coated charcoal-treated fetal bovine serum (DCC-FBS), L-glutamine (1%), 1% antibiotic-antimycotic solution, 2 μg / ml recombinant human insulin and 1nM estradiol. Confluent monolayers were decidualized in DMEM/F-12 containing 2% DCC-FBS (with L-glutamine, excluding insulin

and estrodiol) with 0.5 mM 8-bromo-cAMP (8-br-cAMP; Sigma-Aldrich, Poole, UK) alone or in combination with 1 μM medroxyprogesterone acetate (MPA) to induce a decidual phenotype. Some cultures were also treated with dexamethasone (DEX; 0.1 μM), dihydrotestosterone (DHT, 1 μM) or progesterone (P4, 1 μM). To determine half-life time of *PRIP-1* transcripts, actinomycin D (Sigma-Aldrich) was used at a final concentration of 2 μM in dimethyl sulfoxide (DMSO). All experiments were carried out before the third passage.

Transient transfection

Primary HESCs were transfected using a jetPRIME Polyplus transfection kit (VWR International, Lutterworth, UK). Undifferentiated HESCs were transiently transfected with 50 nM of PRIP-1-siGENOME SMARTpool or siGENOME Non-Targeting (NT) siRNA Pool 1 (Dharmacon, GE Healthcare) for gene knockdown. Transfection studies were performed in triplicate and repeated on primary cultures from 3 or more different biopsies.

Immunohistochemistry and immunofluorescence

Paraffin-embedded, formalin fixed endometrial specimens were immunostained for PRIP-1 using the Novolink polymer detection system (Leica) as per manufacturer's instructions. Universal LSAB Plus Kits (DAKO, Ely, UK) were used as described previously (41) using primary antibodies against PRIP-1 (1:750 dilution; Sigma-Aldrich). As a negative control, the primary antibody was omitted and replaced by the corresponding IgG isotype. For confocal microscopy, primary HESCs were cultured on glass chamber slides (Thermo Scientific, Waltham, MA, USA) and transfected with either NT or PRIP-1 siRNA. HESCs were fixed in 4% paraformaldehyde for 10 min, permeabilized with 0.1% Triton X-100 in TBST for 30 min and blocked in 1% BSA in TBST for 1 hour. Endogenous proteins were stained with rabbit anti-FOXO1 (2880S, 1:100, Cell Signaling Technology), followed by anti-rabbit FITC (F0205,

1:500, DAKO). Cells were mounted in Vectashield with DAPI (Vector Labs, Burlingame, CA, USA) and visualized under a Zeiss LSM 510 META confocal microscope.

Enzyme-linked immunosorbent assay (ELISA)

HESCs were decidualized and lysed in RIPA buffer with protease inhibitors (cOmplete, Mini, EDTA-free; Roche, Welwyn Garden City, UK). PRIP-1 levels in whole cell lysates were determined using a quantitative sandwich ELISA (CusaBio, Wuhan China) according to the manufacturer's protocol. The ELISA was validated by measuring PRIP-1 levels following knockdown and overexpression in cultured human myometrial cells. In spike and recovery experiments, recovered recombinant PRIP-1 within denatured samples was non-significant when compared to spiked concentrations (Supplemental Fig. 1). Furthermore, inter- and intra-assay data variance analysis revealed consistent coefficients of variance (CV) below 5%. Results were derived using a 4-parameter logistic regression analysis and normalised to total protein concentration as determined by Bio-Rad protein assay (Bio-Rad, Hercules, CA, USA).

Real-time quantitative (qRT)-PCR

Total RNA was extracted from HESC cultures using RNA STAT-60 (AMS Biotechnology, Abingdon, UK). Equal amounts of total RNA (1 µg) were treated with DNase and reverse transcribed using the QuantiTect Reverse Transcription Kit (QIAGEN, Manchester, UK). Resulting cDNA was used as a template in qRT-PCR analysis. Detection of gene expression was performed with Power SYBR® Green Master Mix (Life Technologies, Paisley, UK) using the 7500 Real Time PCR System (Applied Biosystems, Foster City, CA, USA). The expression levels of the samples were calculated using the $\Delta\Delta C_T$ method, incorporating the efficiencies of each primer pair. Reaction specificity was confirmed by dissociation curve analysis. *L19* was used as a reference gene for normalization. All measurements were performed in triplicate.

Primer sequences used were as follows: *IGFBP1* forward: 5'-cga agg ctc tcc atg tca cca-3', *IGFBP1* reverse 5'-tgt ctc ctg cct tgg cta aac-3'; *L19* forward 5'-gcg gaa ggg tac agc caa-3', *L19* reverse 5'-gca gcc ggg cgc aaa-3'; *PRIP-1* forward 5'-gca gca gca tca tca agg-3', *PRIP-1* reverse 5'-gct gct gaa aga cac ggt tt-3'; *PRL* forward 5′-aag ctg tag aga ttg agg agc aaa c-3′, *PRL* reverse 5′-tca gga tga acc tgg ctg act a-3′ ; *WNT4* forward 5'- gca gag ccc tca tga acc t-3', *WNT4* reverse 5'-cac cgc atg tgt gtc ag-3'.

Western blot analysis and proteome array

Whole cell protein extracts were prepared by lysing cells in RIPA buffer containing protease inhibitors (cOmplete, Mini, EDTA-free; Roche, Welwyn Garden City, UK). For nuclear and cytoplasmic protein fractionation, cells were lysed in Buffer A (10 mM HEPES, 10 mM KCl, 0.1 mM EDTA), centrifuged at 100 × g, and the supernatant containing the cytoplasmic fraction collected. The remaining pellet was then lysed on ice in high salt buffer (5 mM HEPES, 1.5 mM $MgCl_2$, 0.2 mM EDTA, 300 mM NaCl) for 10 min, centrifuged, and the supernatant, containing the nuclear fraction, retained. Protein yield was measured using the Bradford assay. Equal amounts of protein were separated by SDS-Polyacrylamide Gel Electrophoresis (SDS-PAGE) and wet transfer onto PVDF membrane (GE Healthcare, Buckinghamshire, UK). Nonspecific binding sites were blocked by incubation with 5% non-fat dry milk in Tris-buffered saline with 0.05% Tween (TBS-T; 130 mmol / L NaCl, 20 mmol / Tris, pH 7.6 and 0.05% Tween). The primary antibodies used are tabulated in Table 1. Protein complexes were visualized with ECL Plus chemiluminescence (GE Healthcare). Relative phosphorylation of 26 phospho-kinases was determined by Proteome Profiler Human Phospho-MAPK array kit (R&D Systems, Minneapolis, MN, USA). The array was performed according to manufacturer's specifications using 250 μg total protein lysates. Blots were visualized

following exposure to chemiluminescent reagents and densitometry performed with individual phospho-proteins expressed as a percentage of reference dots.

Confocal imaging of intracellular Ca^{2+} ($[Ca^{2+}]_i$) oscillations

Decidualizing HESCs were washed in modified Krebs'-Henseleit buffer (composition in mmol/l: NaCl 133, KCl 4.7, Glucose 11.1, $MgSO_4$ 1.2, KH_2PO_4 1.2, CaCl 2.5, TES 10; pH 7.4 at 37ºC) and loaded with 5 μM Fluo-4/AM for 1 hour at room temperature (RT). Cells were washed and incubated in 2 ml Krebs'-Henseleit buffer. The glass-bottomed Petri dish containing Fluo-4 loaded cells was secured in a spring-loaded holder in a temperature-controlled environmental chamber on the stage of an inverted microscope (Axiovert 200M) equipped with an LSM 510 META confocal scanner (Karl Zeiss, Cambridge, UK). Cells were excited with a krypton/argon laser at 488 nm and emitted light collected above 510 nm through a 40× oil immersion objective lens. Decidualizing cells transfected with PRIP-1 or non-targeting siRNA were challenged with 5 μM *m*-3M3FBS or vehicle by direct addition into the cell-containing Petri dish. Image sequences of fluo-4 fluorescence were recorded for 10 min at a rate of approximately one frame per second and used as an indication of changes in $[Ca^{2+}]_i$. Videos were analyzed using LSM image analysis software. Averaged fluorescence intensity was measured in regions of interest placed over individual cells and expressed as a fold increase from time 0 (F/F_0). Data traces were plotted and peak response, integral (area under the curve (baseline y=1)) and oscillatory frequency (Hz) were measured.

Viability and proliferation assays

The number of viable cells was assessed by trypan blue exclusion. Cells were counted on the Luna cell counter (Logosbio, Annandale, VA, USA), and percentage viability calculated. Apoptosis was assessed by measurement of the activities of caspase 3/7 using Apo-One

Homogenous kit (Promega, Madison, WI, USA) according to manufacturer's guidelines. Cleavage of a non-fluorescent substrate by caspase 3/7 resulted in fluorescence, measured at 530 nm emission and 490 nm excitation on the PHERAStar FS microplate reader (BMG Labtect, Ortenberg, Germany). Real-time adherent cell proliferation was determined by the label-free xCELLigence Real-Time Cell Analyser (RTCA) DP instrument (Roche Diagnostics GmbH, Basel, Switzerland). HESCs were seeded into 16-well plates (E-plate-16, Roche Diagnostics GmbH) at a density of 10,000 cells per well and cultured in 10 % DCC-FBS until reaching ~80 % confluency. The RTCA DP instrument was placed at 37 °C in a humidified environment with 95 % air and 5 % CO_2. Individual wells within the E-plate-16 were referenced immediately and measured first every 15 min for 3 h and then hourly for 100 h. Changes in cell index were analysed using RTCA Software v1.2.

Statistical Analysis

Data were analysed with the statistical package Graphpad Prism v6 (Graphpad software Inc, La Jolla, CA, USA). Unpaired Student's *t*-test, Mann-Whitney U test and Pearson's correlation were used when appropriate. Statistical significance was assumed at $P < 0.05$. In the actinomycin D experiments, *PRIP-1* mRNA half-life was calculated using $t_{1/2} = 0.693/k$, where k is the slope derived from a linear equation $\ln C = \ln C_0 - kt$, and where C is the relative level of *PRIP-1* mRNA in HESCs (42)

RESULTS

Induction of PRIP-1 in response to progesterone signaling

PRIP-1 mRNA and protein levels were measured in undifferentiated HESCs and cells decidualized for 2, 4, or 8 days (Fig. 1A). Decidualization was associated with marked upregulation of *PRIP-1* transcripts with levels rising > 30 fold within 48 hours of differentiation. The induction of *PRIP-1* mRNA was then maintained over the 8-day time-course. By contrast, induction of PRIP-1 protein was more gradual and expression peaked on day 8 of decidualization (Fig. 1A, lower panel). To define the signaling pathway that drives *PRIP-1* in differentiating HESCs, 3 independent primary cultures were treated with either 8-br-cAMP, MPA or a combination (Fig. 1B). While 8-br-cAMP upregulated *PRIP-1* mRNA levels modestly (~3-fold) after 4 days of treatment, MPA triggered a robust induction (~25-fold). Combined treatment did not yield an additive effect, (Fig. 1B, upper panel) indicating that induction of *PRIP-1* is primarily dependent on progesterone signaling. Regulation at protein level was somewhat divergent as 8-br-cAMP augmented the induction of PRIP-1 in response to MPA treatment (Fig. 1B, lower panel). We speculated that the rise in *PRIP-1* transcripts in decidualizing cells could, at least partly, reflect increased RNA stability. To test this hypothesis, undifferentiated and decidualized HESCs were treated with actinomycin D, a potent transcription inhibitor, for 0.5, 1, 2, 4, or 8 hours. The half-life of *PRIP-1* mRNA in decidualizing cells was non-significantly higher when compared to undifferentiated cells (4.9 versus 3.6 hours, respectively; $P > 0.05$), indicating that the rise in *PRIP-1* is primarily accounted for by progesterone-dependent transcription. MPA is not only a potent activator of the progesterone receptor but also exhibits glucocorticoid- and androgen-like activities in HESCs (43). To determine if *PRIP-1* is indeed a progesterone-responsive gene, primary HESC cultures were treated either with dexamethasone (DEX), dihydrotestosterone (DHT), progesterone (P4), or MPA. As show in Figure 1D, the induction of *PRIP-1* transcripts in

cultures treated with P4 was comparable to the response with MPA. Notably, DHT but not DEX triggered a small but significant increase in *PRIP-1* expression ($P < 0.05$).

Finally, we investigated the expression of PRIP-1 in decidualizing cells upon withdrawal of deciduogenic signals. Parallel cultures were differentiated with 8-br-cAMP and MPA for 4 days. The decidualization stimulus was then withdrawn for 12, 24, 48 or 72 hours and cultures harvested for mRNA and protein analyses. Interestingly, PRIP-1 transcript levels fell by 50% within 24 h after withdrawal of 8-br-CAMP and MPA but then remained stable over the remainder of the time-course (Fig. 1E). By contrast, PRIP-1 protein levels, measured by ELISA, declined only modestly (20%) 72 h after withdrawal of 8-br-cAMP and MPA (Fig. 1F). Taken together, the data reveal a significant lag period between the rapid induction of *PRIP-1* transcript levels in response to progestin signaling and the gradual rise in protein levels. Once induced, PRIP-1 expression is stable and relatively resistant to progesterone withdrawal.

PRIP-1 expression in luteal phase endometrium

Immunohistochemical analysis of mid-luteal endometrial biopsies revealed that PRIP-1 is widely expressed in both the epithelial and stromal compartments (Fig. 2A). PRIP-1 immunoreactivity, however, was heterogeneous, especially in the stromal compartment with some cells staining intensely whereas others showed little expression (Fig. 2A). Mining of the GEO database (GDS2052) revealed that endometrial *PRIP-1* mRNA levels increase markedly during the early-luteal phase, presumably in response to the rapid rise in post-ovulatory progesterone levels. Transcript levels then decline and by the late luteal phase are comparable to proliferative phase endometrium (Fig. 2B). Detailed analysis of timed endometrial biopsies (LH+6 to +10) indicated that PRIP-1 expression is relatively stable over the peri-implantation window. Notably, while transcript levels appeared to decline as the cycle progresses to the late

luteal phase (Spearman's $\rho = -0.1753$, $P = 0.0812$) (Fig. 2C), PRIP-1 protein levels, measured by ELISA, remained stable (Spearman's $\rho = 0.2421$, $P = 0.2437$) (Fig. 2D)

Survival function of PRIP-1 in undifferentiated HESCs.

siRNA-mediated knockdown experiments were performed to examine the function of PRIP-1 in HESCs. Knockdown of this scaffold protein was highly effective; it not only abolished the induction of PRIP-1 in cells decidualized for 4 days but also lowered basal expression in undifferentiated HESCS (Fig. 3A). A trypan blue exclusion assay revealed a 28% reduction in numbers of live cells in undifferentiated HESCs transfected with PRIP-1 siRNA (Fig. 3B). In parallel, caspase-3 and -7 activities increased by > 3-fold (Fig. 3C). Notably, loss of PRIP-1 did not compromise the viability of differentiating cells treated with MPA and 8-br-cAMP (Fig. 3B & C). Real-time monitoring of cell proliferation over 100 h using microelectronic sensor technology (xCELLigence) confirmed that PRIP-1 knockdown completely abolished expansion of undifferentiated HESCs in culture (Fig. 3D). To determine how PRIP-1 exerts its survival function, total protein lysates from HESCs first transfected with NT or PRIP-1 siRNA were hybridized to a proteome array. Analysis of the relative phosphorylation levels of 26 kinases revealed that PRIP-1 knockdown selectively inhibits AKT activation (Fig. 3E). Phosphorylation levels of AKT1 (S473), AKT2 (S474), AKT3 (S472) and pan-AKT (S473, S474, S472) were reduced by 69%, 59%, 46% and 58%, respectively. We speculated that loss of AKT activity upon PRIP-1 knockdown would attenuate FOXO1 turnover by promoting nuclear translocation of this transcription factor (44). Western blot analysis of total protein lysates provided support for this conjecture and further revealed that the increase in FOXO1 levels in undifferentiated HESCs transfected with PRIP-1 coincided with induction of BIM, a well-characterized pro-apoptotic FOXO1 target (Fig. 3F) (45). Analysis of fractionated cytoplasmic and nuclear proteins confirmed that PRIP-1 knockdown increases nuclear FOXO1

levels (Fig. 3G). However, confocal analysis revealed cellular heterogeneity in this response with some stromal cells displaying intense nuclear FOXO1 staining whereas other cells did not (Fig. 3H)

Expression of decidual markers in response to PRIP-1 knockdown.

We next examined if PRIP-1 is important for the expression of decidual marker genes. When compared to cell transfected NT siRNA, knockdown of PRIP-1 prior to decidualization reduced the overall levels of *PRL, IGFBP1, and WNT4* transcripts after 4 days of treatment with 8-br-cAMP and MPA. However, only the reduction in WNT4 mRNA was statistically significant ($P < 0.05$). Furthermore, basal expression of these 3 genes in undifferentiated cells was significantly lower (Fig. 4A). Consequently, the overall responsiveness to deciduogenic signals, determined by fold-induction, was unaffected upon PRIP-1 knockdown; and in case of *PRL* even significantly enhanced (Fig. 4B).

PRIP-1 inhibits PLC-dependent Ca^{2+} signaling

We hypothesised that induction of PRIP-1 in decidualizing cells could serve to silence PLC-dependent Ca^{2+} signaling through PIP2 / IP_3 chelation. To test this conjecture, primary HESCs were transfected with either non-targeting (NT) or PRIP-1 siRNA prior to decidualization for 4 days. The cultures were then loaded with the fluorescent Ca^{2+} indicator Fluo-4 and challenged with the PLC activator *m*-3M3FBS or vehicle (DMSO). Decidualizing cultures transfected with NT siRNA displayed minimal $[Ca^{2+}]_i$ oscillations in response to PLC activation. By contrast, cells transfected with PRIP-1 siRNA exhibited robust and sustained $[Ca^{2+}]_i$ fluxes over the entire recording (Fig. 5A). Analysis of 4 independent cultures revealed PRIP-1 knockdown resulted in 2-fold increase in oscillation frequency, 2-fold increase in peak fluorescence, and 3-fold increase in the area under the curve (Fig. 5B) in response to PLC activation. These results

support the conjecture that the sustained induction of PRIP-1 in decidualizing HESCs acts to sequester phosphoinositides and to limit $[Ca^{2+}]_i$ release.

DISCUSSION

By activating its cognate nuclear receptor, progesterone controls the expression of numerous genes that encode membrane-bound receptors and intermediates in various signal transduction pathways in differentiating HESCs (46,47). Consequently, progesterone transforms the processing of cellular signals and environmental cues upon decidualization. For example, knockdown of PGR is sufficient to inhibit activation of the WNT/beta-catenin, TGFβ/SMAD, and STAT pathways in decidualizing cells (46). Progesterone also induces MAPK phosphatase 1 (MKP-1/DUSP1) (48), which in turn disables JNK and p38 stress-responsive pathways in decidualizing HESCs (49). We now report that progesterone strongly up-regulates PRIP-1 expression in HESCs. Once induced, this scaffold protein accumulates in decidualizing HESCs and levels remain relatively stable even upon withdrawal of progestins.

Unexpectedly, knockdown experiments demonstrated that basal PRIP-1 levels are critical for survival of undifferentiated HESCs. This anti-apoptotic function of PRIP-1 is predicated on its ability to regulate the activity of AKT, either by facilitating interaction with upstream kinases or, conversely, by sequestering AKT phosphatases such as PP2A (50). AKT-dependent phosphorylation of FOXO1 leads to its nuclear export, ubiquitination mediated by E3 ligases such as SKP2 and MDM2, and proteasomal degradation (51,52). PRIP-1 deficiency in HESCs selectively reduced AKT activity by more than 50%, which was sufficient to increase nuclear FOXO1 levels and activate the pro-apoptotic machinery. Notably, loss of cell viability upon PRIP-1 knockdown was only partial. It is increasingly appreciated that primary HESC cultures consist of distinct communities of cells, including clonogenic mesemchymal, mature progeny, perivascular SUSD2-positive cells, and senescent fibroblasts (53-56). Hence, it is not inconceivable that some but not all subpopulations of HESCs are dependent on PRIP-1 for survival, although this conjecture requires further testing.

PRIP-1 knockdown did not interfere with the responsiveness of the HESCs to deciduogenic cues. This is not surprising as FOXO1 accumulates in the nuclei of differentiating HESCs where it binds other decidual transcription factors, including PGR, HOXA11 and C/EBPβ, resulting in formation of transcriptional complexes that activate differentiation genes, including *WNT4*, *PRL* and *IGFBP1* (32,34,35,57). Unexpectedly, basal expression levels of *WNT4*, *PRL* and *IGFBP1* were markedly lower in undifferentiated HESCs transfected with PRIP-1 siRNA. A parsimonious explanation for this intriguing observation is that loss of PRIP-1 triggers apoptosis in a subpopulation of HESCs, characterized by relatively high basal expression of decidual markers. Notably, knockdown of FOXO1 in decidualizing HESC cultures completely eliminates apoptosis upon progestin withdrawal (37,44), indicating that the ability of FOXO1 to switch between apoptosis and differentiation targets is dependent on progesterone signaling.

Upregulation of PRIP-1 in decidual cells may primarily serve to silence PLC signaling downstream of G_q-protein-coupled receptors. Upon implantation, decidual cells form a nutritive matrix for trophoblast invasion that is relatively autonomous and resistant to potentially harmful maternal inputs. Various mechanisms underpinning decidual resistance have been described, including silencing of circadian oscillations (25), massive increase in cellular ROS-scavenging potential (21,23), global cellular hypo-SUMOylation (3,22), and the aforementioned inhibition of stress-responsive pathways (22,58). These adaptations ensure unimpeded progesterone signaling even under conditions of intense tissue remodelling and changing oxygen tension at the feto-maternal interface (22). The trophic function of decidual cells depends on acquisition of a secretory phenotype, which in turn requires rapid expansion of the ER in differentiating HESCs. Ergo, differentiating HESCs mount a physiological

391 unfolded protein response (UPR) characterised by up-regulation of various molecular
392 chaperones, including protein disulfide isomerase (PDI), BIP (GRP78), endoplasmic
393 oxidoreductin-1α (ERO1α), and calnexin (17). We now show that, by chelating IP_3, PRIP-1
394 limits Ca^{2+} release from the expanding ER, which arguably safeguards decidual cells against
395 excessive Ca^{2+} accumulation in the mitochondrial matrix, permeabilization of the
396 mitochondrial outer membrane and subsequent apoptosis (59). Interestingly, PRIP-1 also
397 inhibits autophagosome formation by binding to microtubule-associated protein 1 light chain
398 3 (LC3), a key initiator of the autophagy pathway (60). The importance of these pathways in
399 the endometrium is underscored by recent observations demonstrating that ER stress and
400 autophagy in decidual cells mediate recognition and rejection of developmentally
401 compromised human embryos (17). Arguably, silencing PLC signaling downstream of G_q-
402 protein-coupled receptors may also enhance the biosensoring function of decidual cells by
403 restricting signaling to discrete embryonic cues.
404
405 In conclusion, PRIP-1 is a versatile progesterone-inducible scaffold protein in the
406 endometrium. Our data suggest that the function of PRIP-1 switches from amplifying AKT
407 activity in proliferating HESCs to inhibiting PLC signaling downstream of G_q-protein-coupled
408 receptors in decidual cells. The role of PRIP-1 in regulating the responses of decidual cells to
409 embryonic and trophoblast signals warrants further investigation.
410

Acknowledgement:

This work was supported by the Biomedical Research Unit in Reproductive Health, a joint initiative between the University Hospitals Coventry and Warwickshire NHS Trust and Warwick Medical School. The funder had no role in study design, data collection and analysis, decision to publish, or preparation of the manuscript.

REFERENCES

1. Gellersen B, Brosens JJ. Cyclic decidualization of the human endometrium in reproductive health and failure. Endocr Rev 2014; 35:851-905
2. Bernardini L, Moretti-Rojas I, Brush M, Rojas FJ, Balmaceda JP. Changes in expression of adenyl cyclase activity in human endometrium during hormone replacement therapy and ovarian stimulation. Molecular human reproduction 1999; 5:955-960
3. Jones MC, Fusi L, Higham JH, Abdel-Hafiz H, Horwitz KB, Lam EW, Brosens JJ. Regulation of the SUMO pathway sensitizes differentiating human endometrial stromal cells to progesterone. Proceedings of the National Academy of Sciences of the United States of America 2006; 103:16272-16277
4. Brosens JJ, Hayashi N, White JO. Progesterone receptor regulates decidual prolactin expression in differentiating human endometrial stromal cells. Endocrinology 1999; 140:4809-4820
5. Evans J, Salamonsen LA. Inflammation, leukocytes and menstruation. Rev Endocr Metab Disord 2012; 13:277-288
6. Evans J, Salamonsen LA. Decidualized human endometrial stromal cells are sensors of hormone withdrawal in the menstrual inflammatory cascade. Biol Reprod 2014; 90:14
7. Henriet P, Gaide Chevronnay HP, Marbaix E. The endocrine and paracrine control of menstruation. Mol Cell Endocrinol 2012; 358:197-207
8. Jabbour HN, Kelly RW, Fraser HM, Critchley HO. Endocrine regulation of menstruation. Endocr Rev 2006; 27:17-46
9. Aghajanova L, Horcajadas JA, Weeks JL, Esteban FJ, Nezhat CN, Conti M, Giudice LC. The protein kinase A pathway-regulated transcriptome of endometrial stromal fibroblasts reveals compromised differentiation and persistent proliferative potential in endometriosis. Endocrinology 2010; 151:1341-1355
10. Klemmt PA, Carver JG, Kennedy SH, Koninckx PR, Mardon HJ. Stromal cells from endometriotic lesions and endometrium from women with endometriosis have reduced decidualization capacity. Fertil Steril 2006; 85:564-572
11. Lucas ES, Dyer NP, Murakami K, Lee YH, Chan YW, Grimaldi G, Muter J, Brighton PJ, Moore JD, Patel G, Chan JK, Takeda S, Lam EW, Quenby S, Ott S, Brosens JJ. Loss of Endometrial Plasticity in Recurrent Pregnancy Loss. Stem Cells 2015;
12. Salker M, Teklenburg G, Molokhia M, Lavery S, Trew G, Aojanepong T, Mardon HJ, Lokugamage AU, Rai R, Landles C, Roelen BAJ, Quenby S, Kuijk EW, Kavelaars A, Heijnen CJ, Regan L, Macklon NS, Brosens JJ. Natural selection of human embryos: impaired decidualization of the endometrium disables embryo-maternal interactieons and causes recurrent pregnant loss. PLoS One 2010; April 22
13. Salker MS, Christian M, Steel JH, Nautiyal J, Lavery S, Trew G, Webster Z, Al-Sabbagh M, Puchchakayala G, Foller M, Landles C, Sharkey AM, Quenby S, Aplin JD, Regan L, Lang F, Brosens JJ. Deregulation of the serum- and glucocorticoid-inducible kinase SGK1 in the endometrium causes reproductive failure. Nat Med 2011; 17:1509-1513
14. Salker MS, Nautiyal J, Steel JH, Webster Z, Sucurovic S, Nicou M, Singh Y, Lucas ES, Murakami K, Chan YW, James S, Abdallah Y, Christian M, Croy BA, Mulac-Jericevic B, Quenby S, Brosens JJ. Disordered IL-33/ST2 Activation in Decidualizing Stromal Cells Prolongs Uterine Receptivity in Women with Recurrent Pregnancy Loss. PLoS One 2012; 7:e52252
15. Weimar CH, Kavelaars A, Brosens JJ, Gellersen B, de Vreeden-Elbertse JM, Heijnen CJ, Macklon NS. Endometrial stromal cells of women with recurrent miscarriage fail to discriminate between high- and low-quality human embryos. PLoS One 2012; 7:e41424
16. Weimar CH, Macklon NS, Post Uiterweer ED, Brosens JJ, Gellersen B. The motile and invasive capacity of human endometrial stromal cells: implications for normal and impaired reproductive function. Hum Reprod Update 2013; 19:542-557

17. Brosens JJ, Salker MS, Teklenburg G, Nautiyal J, Salter S, Lucas ES, Steel JH, Christian M, Chan YW, Boomsma CM, Moore JD, Hartshorne GM, Sucurovic S, Mulac-Jericevic B, Heijnen CJ, Quenby S, Koerkamp MJ, Holstege FC, Shmygol A, Macklon NS. Uterine selection of human embryos at implantation. Sci Rep 2014; 4:3894

18. Macklon NS, Brosens JJ. The human endometrium as a sensor of embryo quality. Biol Reprod 2014; 91:98

19. Teklenburg G, Salker M, Molokhia M, Lavery S, Trew G, Aojanepong T, Mardon HJ, Lokugamage AU, Rai R, Landles C, Roelen BA, Quenby S, Kuijk EW, Kavelaars A, Heijnen CJ, Regan L, Brosens JJ, Macklon NS. Natural selection of human embryos: decidualizing endometrial stromal cells serve as sensors of embryo quality upon implantation. PLoS One 2010; 5:e10258

20. Leitao B, Jones MC, Fusi L, Higham J, Lee Y, Takano M, Goto T, Christian M, Lam EW, Brosens JJ. Silencing of the JNK pathway maintains progesterone receptor activity in decidualizing human endometrial stromal cells exposed to oxidative stress signals. Faseb J 2009;

21. Kajihara T, Jones M, Fusi L, Takano M, Feroze-Zaidi F, Pirianov G, Mehmet H, Ishihara O, Higham JM, Lam EW, Brosens JJ. Differential expression of FOXO1 and FOXO3a confers resistance to oxidative cell death upon endometrial decidualization. Mol Endocrinol 2006; 20:2444-2455

22. Leitao BB, Jones MC, Brosens JJ. The SUMO E3-ligase PIAS1 couples reactive oxygen species-dependent JNK activation to oxidative cell death. Faseb J 2011;

23. Sugino N, Karube-Harada A, Kashida S, Takiguchi S, Kato H. Differential regulation of copper-zinc superoxide dismutase and manganese superoxide dismutase by progesterone withdrawal in human endometrial stromal cells. Molecular human reproduction 2002; 8:68-74

24. Sugino N, Karube-Harada A, Sakata A, Takiguchi S, Kato H. Nuclear factor-kappa B is required for tumor necrosis factor-alpha-induced manganese superoxide dismutase expression in human endometrial stromal cells. J Clin Endocrinol Metab 2002; 87:3845-3850

25. Muter J, Lucas ES, Chan YW, Brighton PJ, Moore JD, Lacey L, Quenby S, Lam EW, Brosens JJ. The clock protein period 2 synchronizes mitotic expansion and decidual transformation of human endometrial stromal cells. FASEB journal : official publication of the Federation of American Societies for Experimental Biology 2015; 29:1603-1614

26. Matsuda M, Kanematsu T, Takeuchi H, Kukita T, Hirata M. Localization of a novel inositol 1,4,5-trisphosphate binding protein, p130 in rat brain. Neurosci Lett 1998; 257:97-100

27. Uji A, Matsuda M, Kukita T, Maeda K, Kanematsu T, Hirata M. Molecules interacting with PRIP-2, a novel Ins(1,4,5)P3 binding protein type 2: Comparison with PRIP-1. Life sciences 2002; 72:443-453

28. Yoshida M, Kanematsu T, Watanabe Y, Koga T, Ozaki S, Iwanaga S, Hirata M. D-myo-inositol 1,4,5-trisphosphate-binding proteins in rat brain membranes. J Biochem 1994; 115:973-980

29. Harada K, Takeuchi H, Oike M, Matsuda M, Kanematsu T, Yagisawa H, Nakayama KI, Maeda K, Erneux C, Hirata M. Role of PRIP-1, a novel Ins(1,4,5)P3 binding protein, in Ins(1,4,5)P3-mediated Ca2+ signaling. J Cell Physiol 2005; 202:422-433

30. Fujii M, Kanematsu T, Ishibashi H, Fukami K, Takenawa T, Nakayama KI, Moss SJ, Nabekura J, Hirata M. Phospholipase C-related but catalytically inactive protein is required for insulin-induced cell surface expression of gamma-aminobutyric acid type A receptors. J Biol Chem 2010; 285:4837-4846

31. Sugiyama G, Takeuchi H, Kanematsu T, Gao J, Matsuda M, Hirata M. Phospholipase C-related but catalytically inactive protein, PRIP as a scaffolding protein for phospho-regulation. Adv Biol Regul 2013; 53:331-340

32. Christian M, Zhang X, Schneider-Merck T, Unterman TG, Gellersen B, White JO, Brosens JJ. Cyclic AMP-induced forkhead transcription factor, FKHR, cooperates with CCAAT/enhancer-binding protein beta in differentiating human endometrial stromal cells. J Biol Chem 2002; 277:20825-20832

33. Labied S, Kajihara T, Madureira PA, Fusi L, Jones MC, Higham JM, Varshochi R, Francis JM, Zoumpoulidou G, Essafi A, Fernandez de Mattos S, Lam EW, Brosens JJ. Progestins regulate the expression and activity of the Forkhead transcription factor FOXO1 in differentiating human endometrium. Mol Endocrinol 2005;

34. Takano M, Lu Z, Goto T, Fusi L, Higham J, Francis J, Withey A, Hardt J, Cloke B, Stavropoulou AV, Ishihara O, Lam EW, Unterman TG, Brosens JJ, Kim JJ. Transcriptional cross talk between the forkhead transcription factor forkhead box O1A and the progesterone receptor coordinates cell cycle regulation and differentiation in human endometrial stromal cells. Mol Endocrinol 2007; 21:2334-2349

35. Lynch VJ, Brayer K, Gellersen B, Wagner GP. HoxA-11 and FOXO1A cooperate to regulate decidual prolactin expression: towards inferring the core transcriptional regulators of decidual genes. PLoS One 2009; 4:e6845

36. Lynch VJ, Leclerc RD, May G, Wagner GP. Transposon-mediated rewiring of gene regulatory networks contributed to the evolution of pregnancy in mammals. Nat Genet 2011; 43:1154-1159

37. Labied S, Kajihara T, Madureira PA, Fusi L, Jones MC, Higham JM, Varshochi R, Francis JM, Zoumpoulidou G, Essafi A, Fernandez de Mattos S, Lam EW, Brosens JJ. Progestins regulate the expression and activity of the forkhead transcription factor FOXO1 in differentiating human endometrium. Mol Endocrinol 2006; 20:35-44

38. Matsuda M, Tsutsumi K, Kanematsu T, Fukami K, Terada Y, Takenawa T, Nakayama KI, Hirata M. Involvement of phospholipase C-related inactive protein in the mouse reproductive system through the regulation of gonadotropin levels. Biol Reprod 2009; 81:681-689

39. Chan YW, van den Berg HA, Moore JD, Quenby S, Blanks AM. Assessment of myometrial transcriptome changes associated with spontaneous human labour by high-throughput RNA-seq. Exp Physiol 2014; 99:510-524

40. Brosens JJ, Hayashi N, White JO. Progesterone receptor regulates decidual prolactin expression in differentiating human endometrial stromal cells. Endocrinology 1999; 140:4809-4820

41. Feroze-Zaidi F, Fusi L, Takano M, Higham J, Salker MS, Goto T, Edassery S, Klingel K, Boini KM, Palmada M. Role and regulation of the serum-and glucocorticoid-regulated kinase 1 in fertile and infertile human endometrium. Endocrinology 2007; 148:5020-5029

42. Ross J. MESSENGER-RNA STABILITY IN MAMMALIAN-CELLS. Microbiological Reviews 1995; 59:423-450

43. Africander D, Verhoog N, Hapgood JP. Molecular mechanisms of steroid receptor-mediated actions by synthetic progestins used in HRT and contraception. Steroids 2011; 76:636-652

44. Brosens JJ, Gellersen B. Death or survival--progesterone-dependent cell fate decisions in the human endometrial stroma. Journal of molecular endocrinology 2006; 36:389-398

45. Dijkers PF, Medema RH, Lammers J-WJ, Koenderman L, Coffer PJ. Expression of the pro-apoptotic Bcl-2 family member Bim is regulated by the forkhead transcription factor FKHR-L1. Current Biology 2000; 10:1201-1204

46. Cloke B, Huhtinen K, Fusi L, Kajihara T, Yliheikkilä M, Ho K-K, Teklenburg G, Lavery S, Jones MC, Trew G. The androgen and progesterone receptors regulate distinct gene networks and cellular functions in decidualizing endometrium. Endocrinology 2008; 149:4462-4474

47. Gellersen B, Brosens JJ. Cyclic Decidualization of the Human Endometrium in Reproductive Health and Failure. Endocrinology Review 2014;

48. Chen C-C, Hardy DB, Mendelson CR. Progesterone receptor inhibits proliferation of human breast cancer cells via induction of MAPK phosphatase 1 (MKP-1/DUSP1). Journal of Biological Chemistry 2011; 286:43091-43102

49. Leitao B, Jones MC, Fusi L, Higham J, Lee Y, Takano M, Goto T, Christian M, Lam EWF, Brosens JJ. Silencing of the JNK pathway maintains progesterone receptor activity in decidualizing human endometrial stromal cells exposed to oxidative stress signals. Faseb Journal 2010; 24

50. Sugiyama G, Takeuchi H, Kanematsu T, Gao J, Matsuda M, Hirata M. Phospholipase C-related but catalytically inactive protein, PRIP as a scaffolding protein for phospho-regulation. Advances in biological regulation 2013; 53:331-340

51. Huang H, Tindall DJ. Regulation of FOXO protein stability via ubiquitination and proteasome degradation. Biochimica et Biophysica Acta (BBA)-Molecular Cell Research 2011; 1813:1961-1964

52. Huang H, Regan KM, Wang F, Wang D, Smith DI, van Deursen JMA, Tindall DJ. Skp2 inhibits FOXO1 in tumor suppression through ubiquitin-mediated degradation. Proceedings of the National Academy of Sciences of the United States of America 2005; 102:1649-1654

53. Lucas ES, Dyer NP, Murakami K, Hou Lee Y, Chan YW, Grimaldi G, Muter J, Brighton PJ, Moore JD, Patel G. Loss of Endometrial Plasticity in Recurrent Pregnancy Loss. STEM CELLS 2015;

54. Murakami K, Lee YH, Lucas ES, Chan Y-W, Durairaj RP, Takeda S, Moore JD, Tan BK, Quenby S, Chan JKY. Decidualization induces a secretome switch in perivascular niche cells of the human endometrium. Endocrinology 2014; 155:4542-4553

55. Kusama K, Yoshie M, Tamura K, Kodaka Y, Hirata A, Sakurai T, Bai H, Imakawa K, Nishi H, Isaka K. Regulation of decidualization in human endometrial stromal cells through exchange protein directly activated by cyclic AMP (Epac). Placenta 2013; 34:212-221

56. Gargett CE, Schwab KE, Deane JA. Endometrial stem/progenitor cells: the first 10 years. Human reproduction update 2015:dmv051

57. Vasquez YM, Mazur EC, Li X, Kommagani R, Jiang L, Chen R, Lanz RB, Kovanci E, Gibbons WE, DeMayo FJ. FOXO1 is required for binding of PR on IRF4, novel transcriptional regulator of endometrial stromal decidualization. Molecular endocrinology 2015; 29:421-433

58. Leitao B, Jones MC, Fusi L, Higham J, Lee Y, Takano M, Goto T, Christian M, Lam EW, Brosens JJ. Silencing of the JNK pathway maintains progesterone receptor activity in decidualizing human endometrial stromal cells exposed to oxidative stress signals. Faseb J 2010; 24:1541-1551

59. Deniaud A, Sharaf el dein O, Maillier E, Poncet D, Kroemer G, Lemaire C, Brenner C. Endoplasmic reticulum stress induces calcium-dependent permeability transition, mitochondrial outer membrane permeabilization and apoptosis. Oncogene 2008; 27:285-299

60. Umebayashi H, Mizokami A, Matsuda M, Harada K, Takeuchi H, Tanida I, Hirata M, Kanematsu T. Phospholipase C-related catalytically inactive protein, a novel microtubule-associated protein 1 light chain 3-binding protein, negatively regulates autophagosome formation. Biochemical and biophysical research communications 2013; 432:268-274

FIGURE LEGENDS

Figure 1. Progesterone regulates *PRIP-1* expression in HESCs. (A) PRIP-1 transcript and protein levels were measured in undifferentiated HESCs and cells decidualized with 8-br-cAMP and MPA for 2, 4, or 8 days. The upper panel shows fold induction of *PRIP-1* mRNA (mean ± SEM) in 3 independent primary cultures relative to expression in undifferentiated cells. Total protein lysates from parallel cultures were subjected to Western blotting (lower panel). β-Actin served as a loading control. (B) Primary HESC cultures were treated with either 8-br-cAMP, MPA or a combination for 96 hours. The upper panel shows the relative increase in *PRIP-1* mRNA levels (mean ± SEM) compared to vehicle-treated undifferentiated HESC cultures established from 3 biopsies. The lower panel shows the corresponding protein levels, determined by Western blotting. β-Actin served as a loading control. (C) Primary cultures (n = 3) remained undifferentiated or were decidualized for 96 h prior to treatment with 2 μM actinomycin D. RNA was extracted at the indicated time points and subjected to qRT-PCR analysis. (D) Primary HESCs isolated from 3 different biopsies were treated with dexamethasone (DEX), dihydrotestosterone (DHT), progesterone (P4), MPA or vehicle (control). Total RNA was harvested 96 hours later and subjected to qRT-PCR analysis. The data show induction of *PRIP-1* transcripts (mean ± SEM) relative to control cells. (E) *PRIP-1* transcripts were measured following withdrawal of MPA for the indicated time-points in 3 separate cultures first decidualized with 8-br-cAMP and MPA for 96 h. *PRIP-1* mRNA levels were normalised to the level of expression in undifferentiated cells (dotted line). (F) Total protein lysates were harvested from parallel cultures PRIP-1 protein levels determined by ELISA. * denotes $P < 0.05$, ** $P < 0.01$

Figure 2. PRIP-1 expression in mid-luteal endometrium. (A) Immunohistochemistry of mid-luteal endometrial biopsies demonstrates heterogeneous expression of PRIP-1 in both stromal and epithelial cells. (B) Comparison of endometrial *PRIP-1* transcripts, expressed in arbitrary units (A.U.), in proliferative, early-, mid-, and late-secretory endometrium. The data were derived from *in silico* analysis of publicly available microarray data (GEO Profiles; ID: GDS2052). * denotes $P < 0.05$. (C) *PRIP-1* transcript levels were measured by qRT-PCR in 73 endometrial biopsies obtained between 6 and 10 days after the LH surge (LH+). (D) PRIP-1 protein levels were measured, in triplicate, in 25 whole endometrial samples by ELISA.. Dotted lines represent 95% confidence intervals.

Figure 3. PRIP-1 is a survival factor in undifferentiated HESCs. (A) Three independent primary cultures were transfected with either non-targeted (NT) or PRIP-1 siRNA. After 48 hours, some cultures were decidualized for 96 h whereas others remained untreated. PRIP-1 mRNA and protein levels were measured in parallel cultures by qRT-PCR (upper panel) and Western blot (lower panel), respectively. Transcript levels were normalized to expression in undifferentiated cells transfected with NT siRNA. *** denotes $P < 0.001$. (B) Cell viability as measured by trypan blue exclusion assay in 3 independent primary cultures first transfected with either NT or PRIP-1 siRNA. Following transfection, the cultures remained either untreated or were decidualized for 96 h. Data normalised to un-transfected control (dotted line) (C) In parallel experiments, caspase 3/7 activity was measured and expressed in fluorescent intensity units (F.I.U). The data represent mean (± SEM) activity in 3 independent cultures. ** denotes $P < 0.01$. (D) Real-time monitoring of the growth of undifferentiated HESCs over 100 h following transfection with NT or PRIP-1 siRNA. (E) Protein lysates from undifferentiated HESC transfected with either NT or PRIP-1 siRNA were subjected to Proteome Profiler MAPK array membranes and analysed by densitometry. * denotes $P < 0.05$ and *** $P < 0.01$. (F)

Western blot analysis of total protein lysates from undifferentiated HESCs 48 h following transfection with either NT or PRIP-1 siRNA. (G) Nuclear accumulation of FOXO1 was confirmed by Western blot analysis of cytoplasmic and nuclear cell fractions. VINCULIN and LAMIN A/C confirmed enrichment of the cytoplasmic and nuclear proteins, respectively. (H) Confocal microscopy showing FOXO1 immunoreactivity in primary HESCs transfected with either NT or PRIP-1 siRNA. Arrow heads indicate cells characterized by marked nuclear FOXO1 accumulation.

Figure 4. PRIP-1 blunts the overall expression of differentiation markers in decidualizing HESCs (A) Three independent primary HESCs were first transfected with NT or PRIP-1 siRNA. The cultures then remained untreated or were decidualized with 8-br-cAMP and MPA. The data shows relative expression (mean ± SEM) of decidual marker genes. (B) The same data expressed as fold-induction in transcript level relative to the basal levels in undifferentiated cells transfected with NT or PRIP-1 siRNA. * denotes $P < 0.05$ and *** $P < 0.01$.

Figure 5. PRIP-1 blocks PLC-dependent Ca^{2+} signaling in decidual cells. (A) HESCs cultured in glass bottomed petri-dishes were transfected with NT (left panel) or PRIP-1 (right panel) siRNA and decidualized for 4 days. Cells were then loaded with 5 μM Fluo-4-AM and challenged with 5μM *m*-3M3FBS or vehicle (data not shown) at the indicated time-point. Cytosolic fluorescence recorded by confocal microscopy over 10 min was used as an index of $[Ca^{2+}]_i$. Traces showing fluorescence within individual cells, transfected either with NT (left panel) or PRIP-1 siRNA (right panel) are expressed as a fold increase over fluorescence at time-0 (F/F_0). Data were obtained from 4 independent cultures. (B) Traces were analysed to

675 assess the peak changes in fluorescence, the integral, and oscillation frequency (Hz). Data show

676 mean ± SEM. **** denotes $P < 0.0001$.

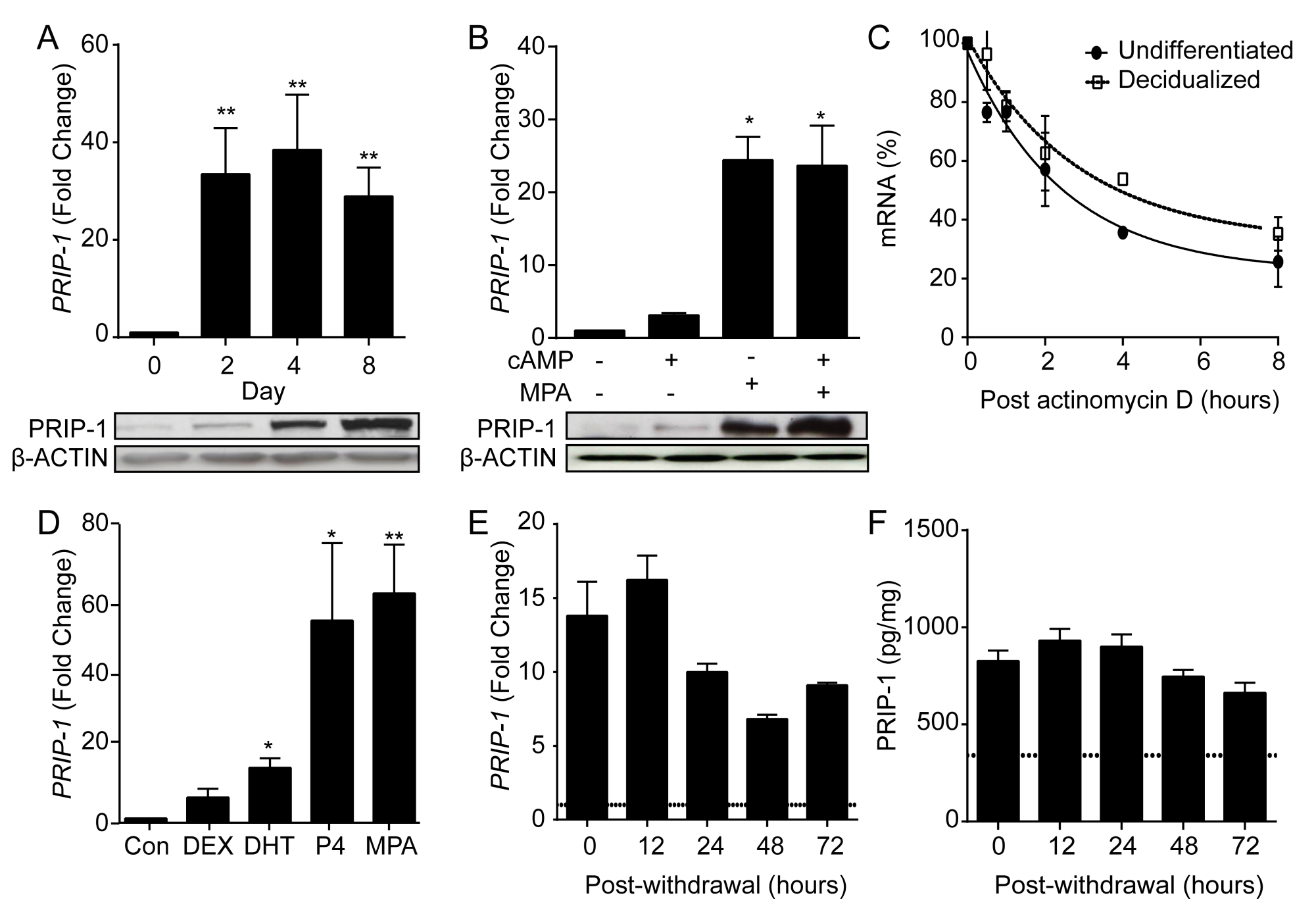
A
PRIP-1 (Fold Change)
60
40
20
0
**
**
**
0
2
4
8
Day
PRIP-1
β-ACTIN
B
PRIP-1 (Fold Change)
40
30
20
10
0
*
*
cAMP - + - +
MPA - - + +
PRIP-1
β-ACTIN
C
mRNA (%)
100
80
60
40
20
0
Undifferentiated
Decidualized
0
2
4
6
8
Post actinomycin D (hours)
D
PRIP-1 (Fold Change)
80
60
40
20
0
*
*
Con
DEX
DHT
P4
MPA
E
PRIP-1 (Fold Change)
20
15
10
5
0
0
12
24
48
72
Post-withdrawal (hours)
F
PRIP-1 (pg/mg)
1500
1000
500
0
0
12
24
48
72
Post-withdrawal (hours)

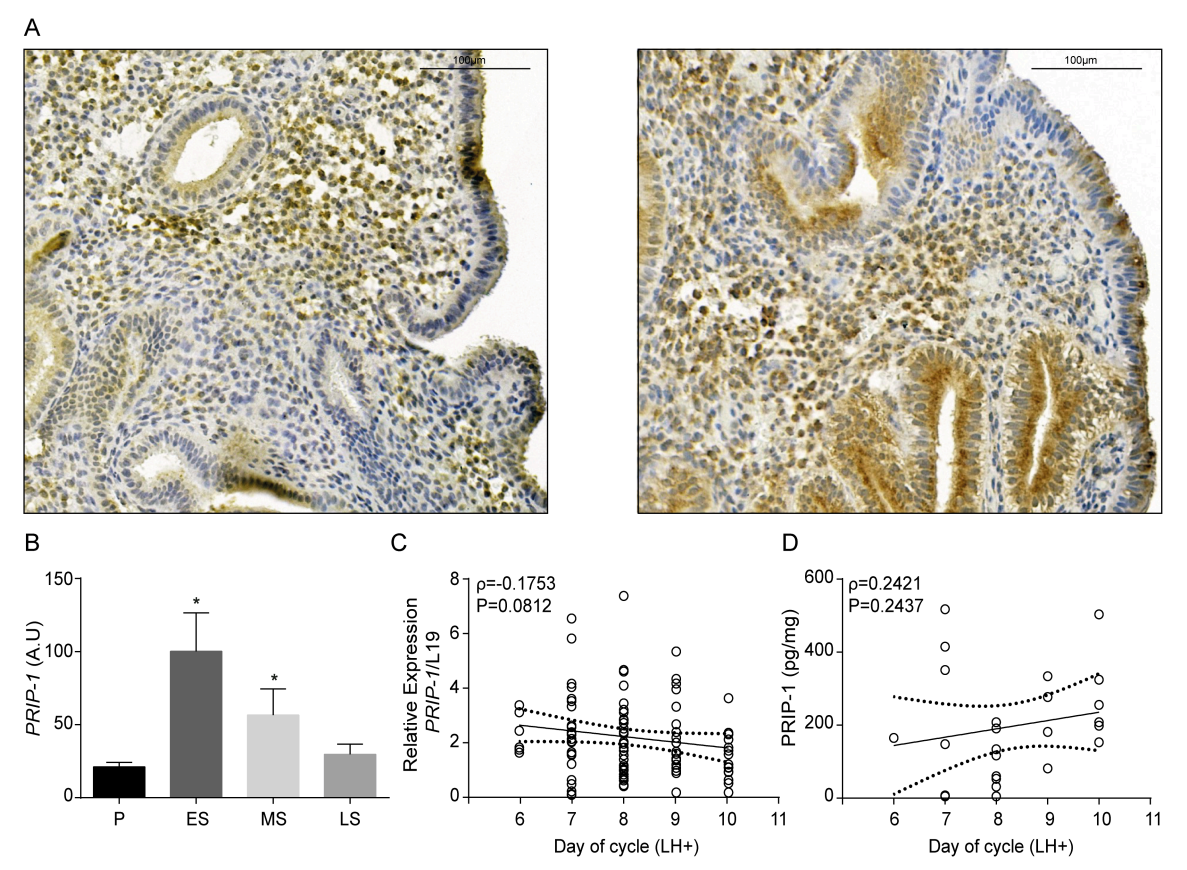
A
100µm
100µm
B
PRIP-1 (A.U)
150
100
50
0
*
*
P
ES
MS
LS
C
Relative Expression
PRIP-1/L19
ρ=-0.1753
P=0.0812
8
6
4
2
0
6
7
8
9
10
11
Day of cycle (LH+)
D
PRIP-1 (pg/mg)
ρ=0.2421
P=0.2437
600
400
200
0
6
7
8
9
10
11
Day of cycle (LH+)

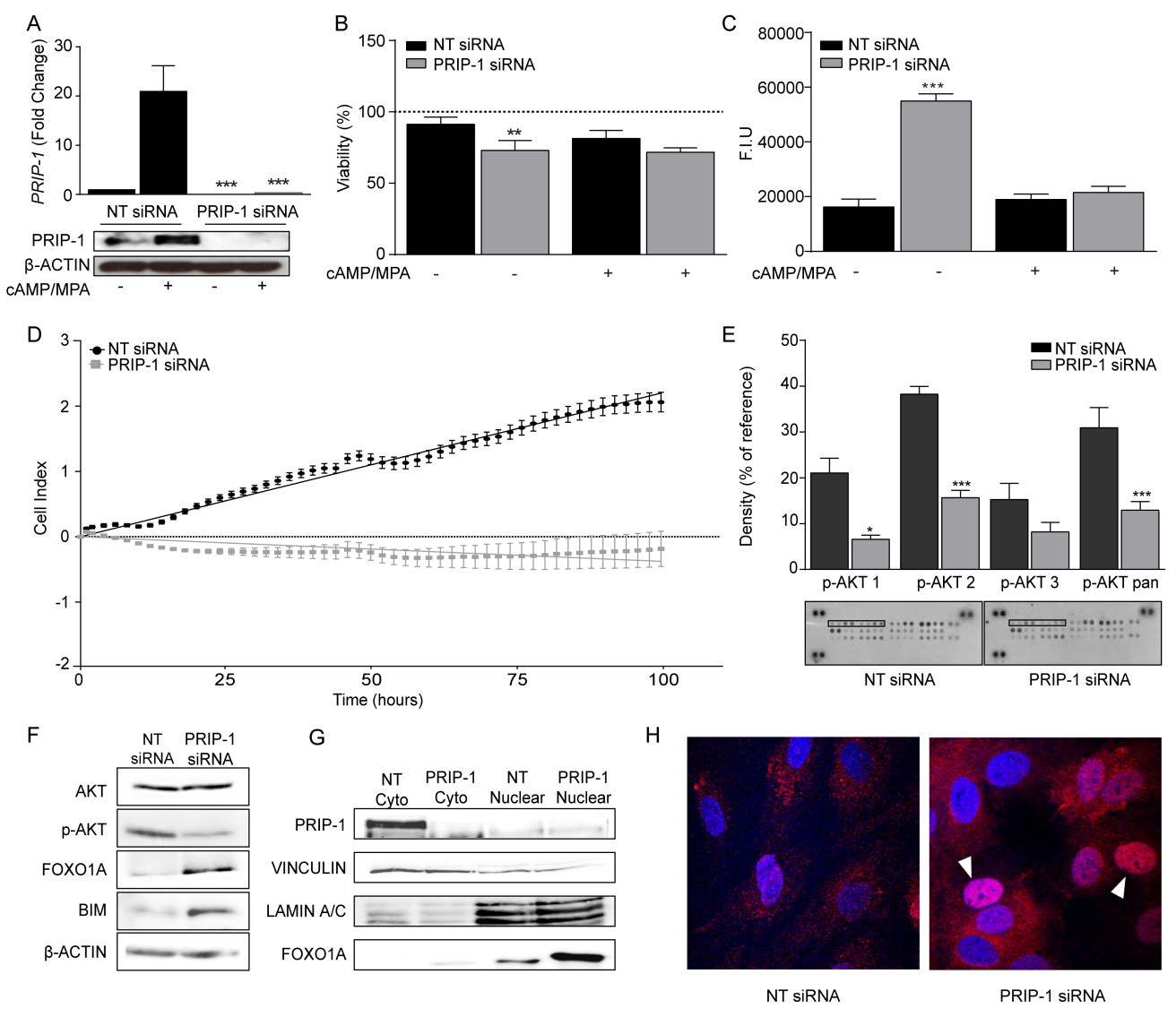
A
PRIP-1 (Fold Change)
30
20
10
0
***
***
NT siRNA
PRIP-1 siRNA
PRIP-1
β-ACTIN
cAMP/MPA
- + - +
B
150
100
50
0
Viability (%)
NT siRNA
PRIP-1 siRNA
**
cAMP/MPA - - + +
C
80000
60000
40000
20000
0
F.I.U
NT siRNA
PRIP-1 siRNA
***
cAMP/MPA - - + +
D
NT siRNA
PRIP-1 siRNA
Cell Index
3
2
1
0
-1
-2
0
25
50
75
100
Time (hours)
E
50
40
30
20
10
0
Density (% of reference)
NT siRNA
PRIP-1 siRNA
*
***
***
p-AKT 1
p-AKT 2
p-AKT 3
p-AKT pan
NT siRNA
PRIP-1 siRNA
F
NT siRNA
PRIP-1 siRNA
AKT
p-AKT
FOXO1A
BIM
β-ACTIN
G
NT Cyto
PRIP-1 Cyto
NT Nuclear
PRIP-1 Nuclear
PRIP-1
VINCULIN
LAMIN A/C
FOXO1A
H
NT siRNA
PRIP-1 siRNA

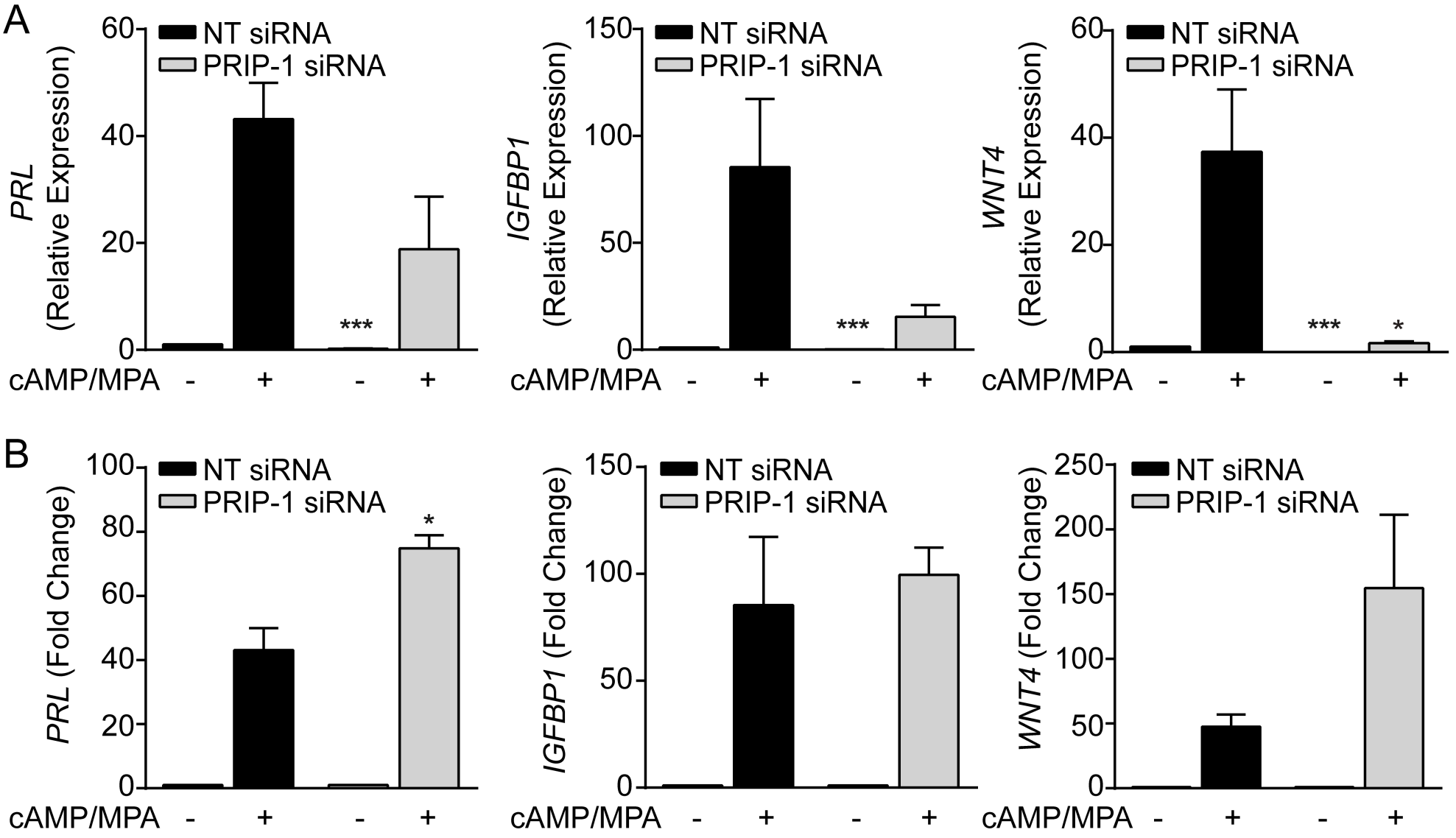
A
PRL (Relative Expression)
IGFBP1 (Relative Expression)
WNT4 (Relative Expression)
NT siRNA
PRIP-1 siRNA
cAMP/MPA
***
*
B
PRL (Fold Change)
IGFBP1 (Fold Change)
WNT4 (Fold Change)

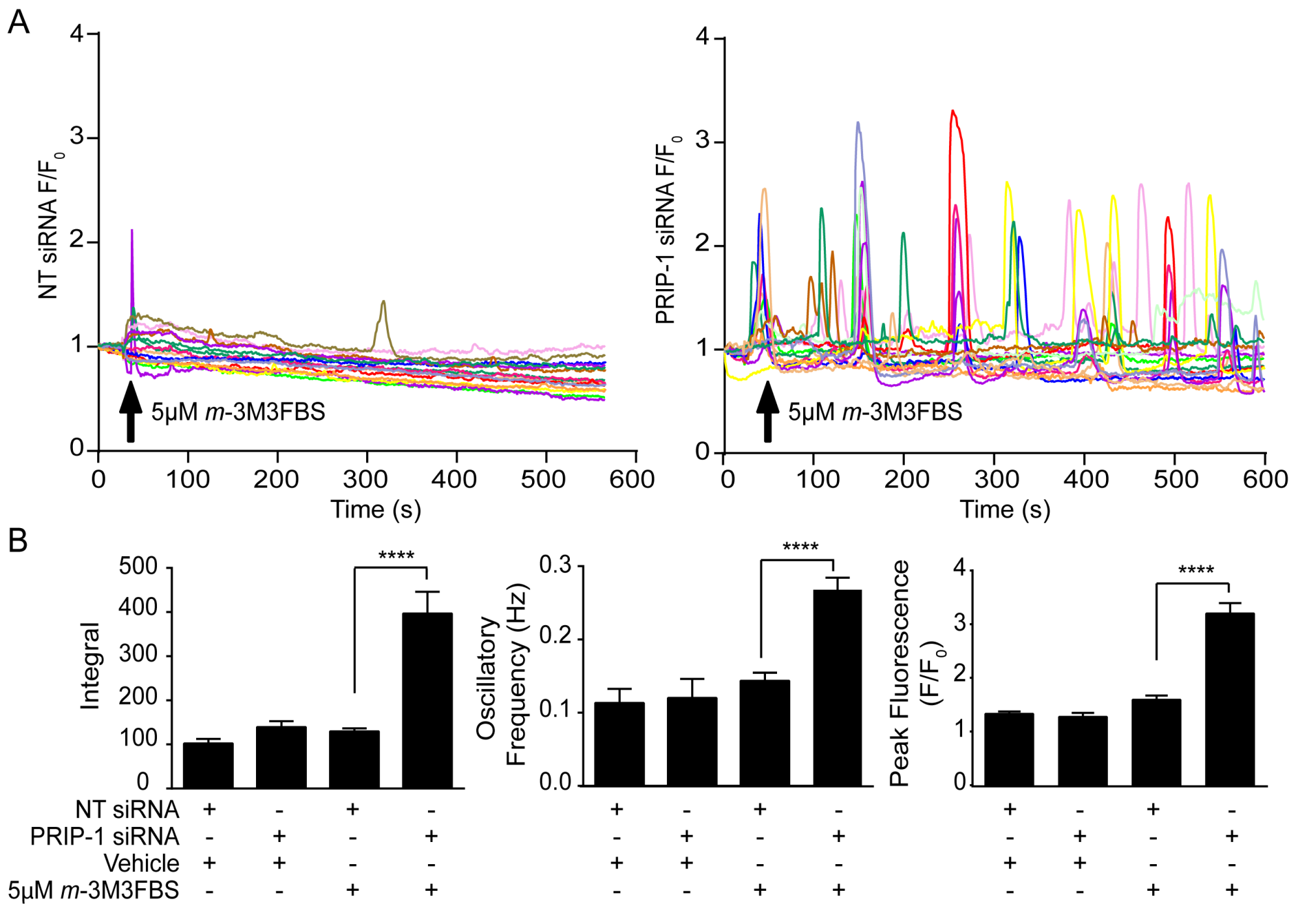
A
NT siRNA F/F0
PRIP-1 siRNA F/F0
5μM m-3M3FBS
Time (s)
B
Integral
Oscillatory Frequency (Hz)
Peak Fluorescence (F/F0)
****
NT siRNA
PRIP-1 siRNA
Vehicle
5μM m-3M3FBS

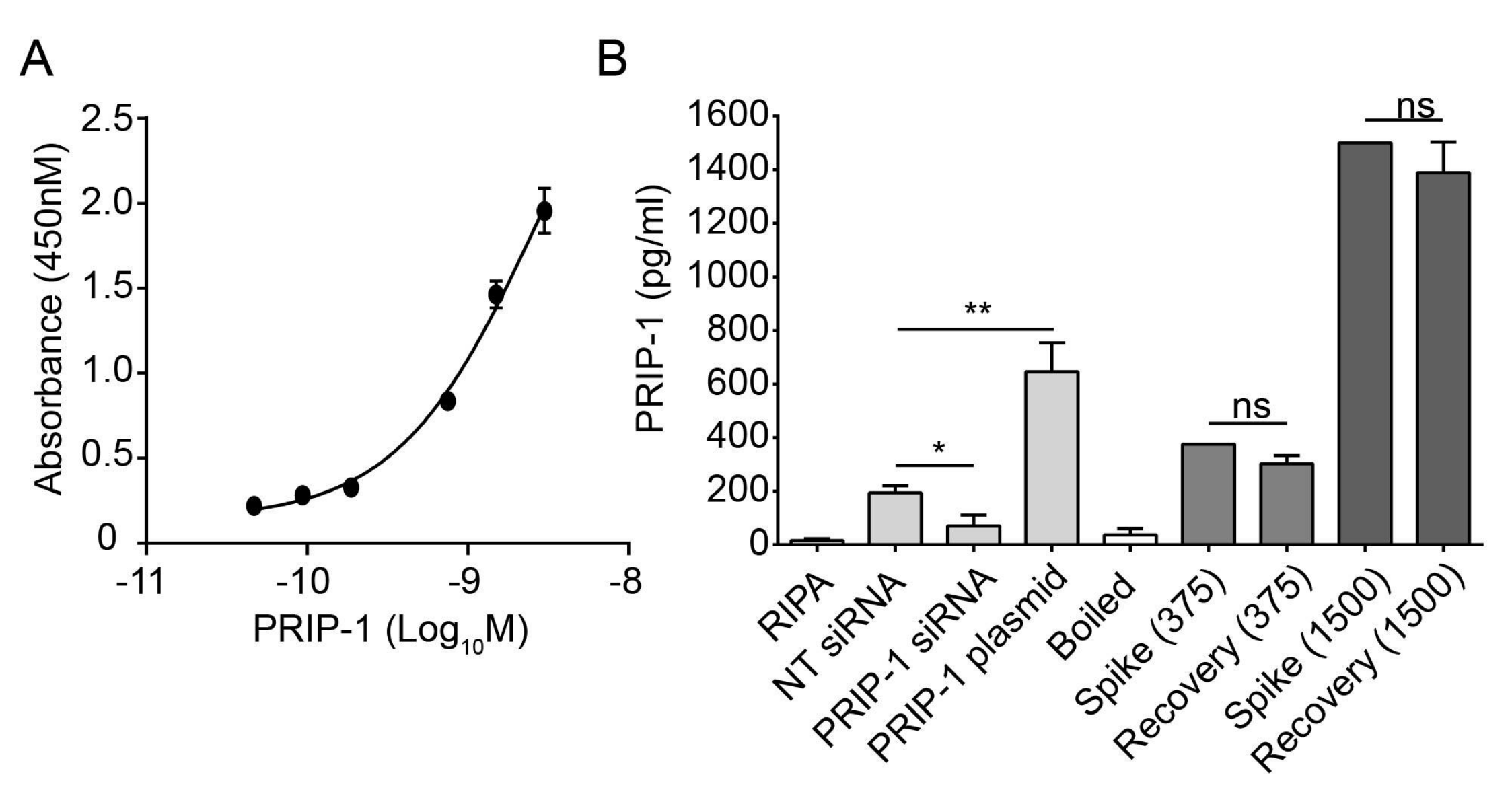
A
Absorbance (450nM)
2.5
2.0
1.5
1.0
0.5
0
-11
-10
-9
-8
PRIP-1 (Log10M)
B
PRIP-1 (pg/ml)
1600
1400
1200
1000
800
600
400
200
0
**
*
ns
ns
RIPA
NT siRNA
PRIP-1 siRNA
PRIP-1 plasmid
Boiled
Spike (375)
Recovery (375)
Spike (1500)
Recovery (1500)

Supplemental Fig. 1. Validation of PRIP-1 Sandwich ELISA. For generation of the PRIP-1 standard curve (A), supplied recombinant PRIP-1 was diluted and assayed exactly as per ELISA manufacturer's instructions (CusaBio, Wuhan, China). (B) To validate the ELISA, cultured primary myometrial cells were transfected with either 50 nM PRIP-1 siRNA, non-targeting (NT) scrambled siRNA controls, or 1 µg plasmid DNA encoding the PRIP-1 gene. PRIP-1 plasmid DNA was purified from ready-transformed bacterial glycerol stocks containing the cDNA for human PRIP-1 in a pCR4-TOPO plasmid (Thermo Scientific, Hemel Hempstead, UK). Cells were transfected via an Amaxa™ basic Nucleofector™ kit as per manufacturer's instructions (Lonza, Basel, Switzerland), lysed and assayed for PRIP-1 content. In spike and recovery experiments, recombinant PRIP-1 was spiked into denatured (30 min, 100^{o}C) myometrial cell lysates and recovered PRIP-1 levels determined. Spike and recovery experiments revealed no significant differences. Data are mean ± SEM., n=3.

Table 1: Primary Antibodies

Protein Target	Manufacturer	Dilution
PRIP-1	Sigma- Aldrich (HPA031849)	WB 1:500 Immunohistochemistry 1:750
AKT	Cell Signaling Technology (4691)	WB 1:1000
p-AKT (Ser473)	Cell Signaling Technology (4060)	WB 1:1000
FOXO1A	Cell Signaling Technology (2880)	WB 1:1000
BIM	Cell Signaling Technology (2933)	WB 1:1000
VINCULIN	Abcam (ab18058)	WB 1:1000
LAMIN A/C	Santa-Cruz Biotechnology (sc-7292)	WB 1:500
β-ACTIN	Abcam (ab8226)	WB 1:10,000